Stress among the APS-Prepared TBCs: Testing and Analysis

Zhaoliang Qu, Rujie He and Daining Fang

Abstract

Stress state in thermal barrier coatings (TBCs) has an influence on the service property and safety of coatings. The stress in TBCs should be characterized and measured. This is helpful for the guidance of design and preparation, the study of failure mechanism and the promotion of application of TBCs. This chapter reviewed the research progress on the stress measurement for air plasma spray (APS)-prepared TBCs. The origin and category of stress during preparation process and service were discussed. Then, the measurement technology and characterization method for stress in APS-prepared TBCs were focused. The common stress measurement techniques such as X-ray diffraction, neutron diffraction, Raman spectroscopy, photoluminescence piezospectroscopy, curvature measurement, material removal and indentation method were detailed. Furthermore, some suggestions were presented for the future work by summarizing the shortcomings of the exiting research.

Keywords: air plasma spray process, thermal barrier coatings, stress testing, stress analysis

1. Introduction

Gas-turbine engine, which is known as the heart of aircraft, covers many leading-edge technologies in advanced manufacturing industry, and represents the level of a nation's science and technology. Higher thrust-weight ratio, longer service lifetime and better reliability are regarded as the development trend for the gas-turbine engine. Increasing the turbine inlet temperature is an important method for increasing the thrust-weight ratio. Key technologies for increasing the turbine inlet temperature include single crystal superalloy, air cooling and thermal barrier coatings (TBCs) technology. Specially, TBCs can lower the operating temperature of superalloy blade. The temperature reduction caused by TBCs is equal to the sum of temperature rise induced by superalloy over the last 30 years. Besides, TBCs can protect the metallic blade from oxidizing, and improve the service safety and lifetime of the blade [1–3].

Among traditional TBCs, porous ceramics with low thermal conductivity are prepared on superalloy substrate to achieve heat insulation effect. But the mismatch of thermo-mechanical properties between porous ceramics and superalloy leads to the difficulty in reliable bonding. A bond coat is necessary [2]. Thus, TBCs is a typical multilayer, multi-material system, as shown in **Figure 1**. TBCs mainly include (1) the ceramic top coat, (2) the thermally grown oxide (TGO), (3) the bond coat, and (4) superalloy substrate. The ceramic top coat usually adopts porous ceramics to achieve heat insulation effect. The common ceramic composition is the zirconia
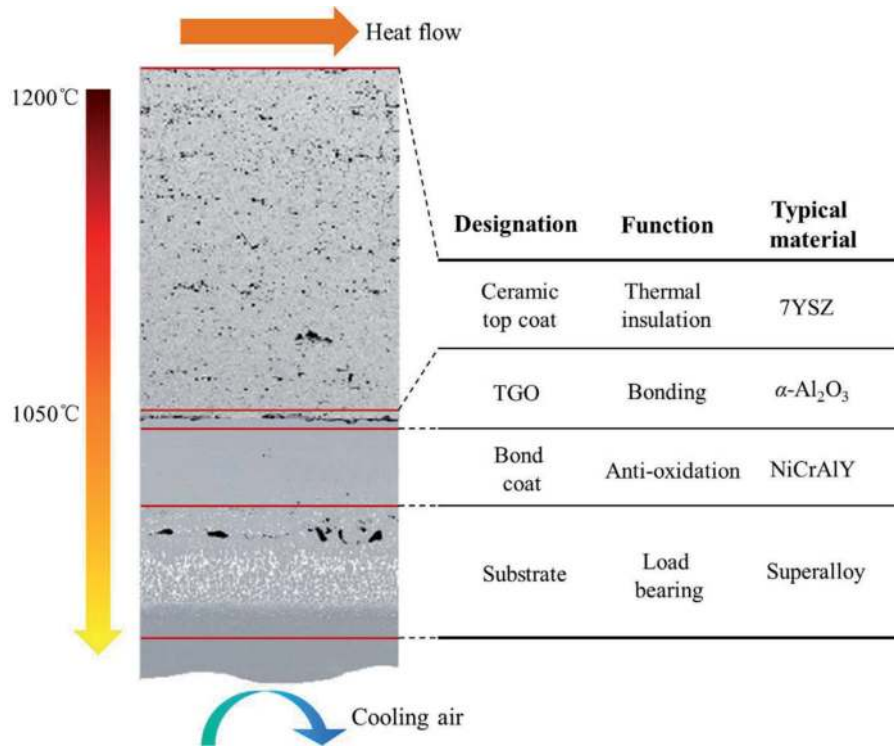
Figure 1.
The schematic of typical TBCs.

'partially stabilized' with about 6–8 wt.% yttria (7YSZ), which has the good heat-insulating property and long thermal cycle life. TGO, whose composition is α-Al$_2$O$_3$, is formed by the reaction between aluminum diffusing from the bond coat and exterior oxygen. TGO can provide good bonding of TBC to bond coat. The bond coat contains the source of elements to create TGO in oxidizing environment and provides oxidation protection, primarily of NiCoCrAlY- or NiAlPt-based compositions. The superalloy substrate, which has high strength at high temperatures, can experience complicated mechanical loads during service [1, 2, 4].

Recently, many methods have been developed to prepare the ceramic top coat, such as air plasma spray (APS) and electron beam physical vapor deposition (EB-PVD) process [5, 6]. In APS process, the ceramic feedstock are injected into the high temperature plasma plume, heated to the molten or high-plasticity condition, impinge onto the surface of specimen with a certain momentum, and rapidly solidify. Then the lamellar microstructures, which consist of a large number of overlapped splats, are formed, as shown in **Figure 2(a)**. In EB-PVD process, ingots of a ceramic composition are vaporized in a vacuum chamber using a focused electron beam. The ceramic vapor gradually deposit on the specimen and form columnar microstructure, which are perpendicular to the surface of specimen, as shown in **Figure 2(b)**.

TBCs prepared by APS process, which has lower cost, has been widely used in the larger stationary components. However, the failure behavior such as premature spallation of TBCs during preparation and operation process is still an overriding concern. The premature spallation of TBCs may expose the superalloy substrate to hot gases, resulting in the oxidization of superalloy. This may influence the service performance, lifetime and safety of aircraft, even lead to catastrophic damage [7]. The premature spallation of TBCs mainly results from intralayer and interlayer fractures [8]. The fracture behavior of materials is closely related to stress state. When the stress in a material is tensile, and is larger than strength, the fracture behavior may happen. The change of stress state is considered as the driving force
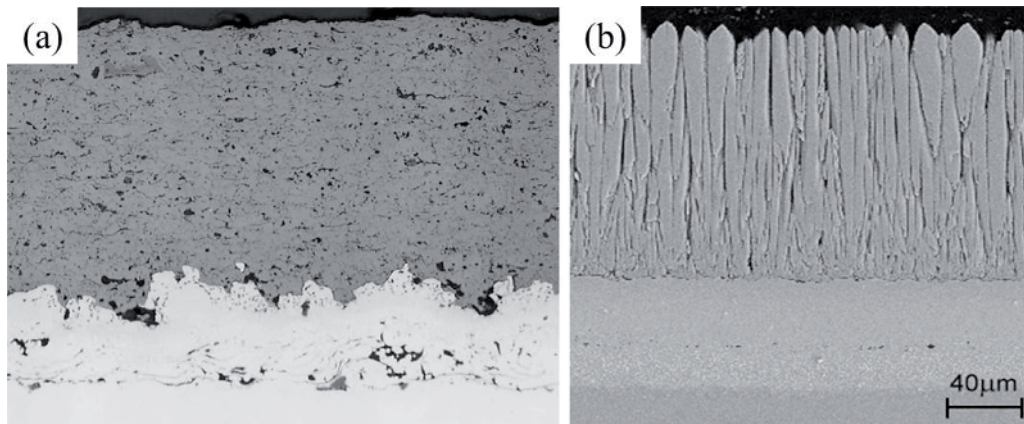
Figure 2.
The microstructures of TBCs prepared by: (a) APS and (b) EB-PVD.

for the initiation, propagation of cracks [9]. Besides, the stress state may influence the macroscopic properties of TBCs [10]. Specially, the microstructures of TBCS prepared by APS process are typical lamellar microstructures. The lamellar microstructures may not totally melt and bond each other. There are a large number of defects such as pores and microcracks between lamellar microstructures [11]. As the defects are sensitive to stress state, the material near the defects tends to fracture under stress, leading to the spallation of coatings. Therefore, the analysis and characterization of stress in TBCs prepared by APS process is necessary for the study of failure mechanism and service reliability.

This chapter reviews the research progress on the analysis and characterization of stress among the APS-prepared TBCs in recent years. The origin, category, measurement technology and characterization method for stress are focused. It is believed this will be helpful for the investigation on failure mechanism, and promote the application and development of TBCs.

2. The origin and category of stress among the APS-prepared TBCs

TBCs experiences complicated loads during the preparation process and service. Then, stress state in TBCs dynamically changes and influences the service properties and behaviors of TBCs.

2.1 The origin and category of stress during preparation process

In APS process, the molten ceramic feedstock impinge onto the surface of metal specimen, stack and form TBCs [12]. The coatings may experience violent temperature change in the process. The mismatch of thermal expansion coefficients between ceramics layer and superalloy may produce stress [13]. According to the mechanism of stress generation, the stress generating in preparation process mainly includes quenching stress and thermal mismatch stress, as shown in **Figure 3**.

The quenching stress is generated in the interaction process between molten ceramic feedstock and metal specimen. In this process, the feedstock after impact may form a lamellar structure and rapidly cool from the molten temperature to the specimen temperature in a short time. The lamellar structure shrinks sharply due to rapid cooling. The shrinkage of the newly formed lamellar structure is constrained by the specimen and the previous lamellar structure, resulting in stress in the coating [14]. The constraint of the specimen and the previous lamellar structure depends
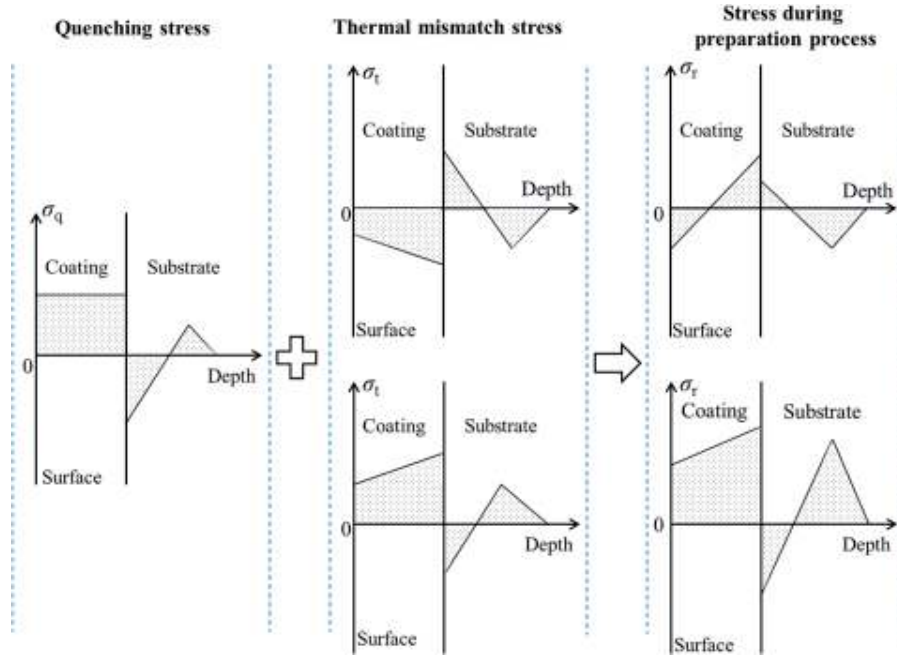
Figure 3.
The stresses during preparation process of APS-prepared TBCs.

mainly on the material of the lamellar structure, the temperature of the specimen, and the boundary shapes between the lamellar structures [15]. The existence of quenching stress has been proven by McPherson, and the value has been measured by Kuroda et al. It is found that the quenching stress is always tensile stress [16, 17]. Assuming that the shrinkage deformation of the lamellar structure is fully constrained, the resulting stress will be large, and much higher than the yield strength or fracture strength of the material. The maximum value of quenching stress given by the elastic mechanics analysis is about 1 GPa, while the values obtained from the experiments are mostly below 100 MPa. This is mainly due to the existence of many stress release mechanisms during the preparation of the coating. For example, a large number of microcracks are generated inside and at the boundary of the lamellar structure during the preparation process. These microcracks can act as important means of stress release, reducing stress below the fracture strength [13, 18].

The thermal mismatch stress generates during the cooling process after spraying. The thermal mismatch stress results from the mismatch of thermal expansion coefficients between the ceramic coating and the metal specimen [9, 19]. In the elastic range, the thermal mismatch stress can be estimated by:

$$\Delta \varepsilon_{th} = \int_{T_2}^{T_1}(\alpha_1(T) - \alpha_2(T))dT \tag{1}$$

$$\sigma_{th}(T) = \Delta \varepsilon_{th} E(T) \tag{2}$$

where, $\Delta \alpha (T)$ is the difference in thermal expansion coefficients between ceramic coating and metal material, and changes with temperature. T_1 is the spray temperature. T_2 is the certain temperature during the cooling process. $\sigma_{th}(T)$ is the thermal mismatch stress of coatings. $E(T)$ is the elastic modulus of coating material. According to Eqs. (1) and (2), the thermal mismatch stress is related to the difference in thermal expansion coefficients, the spray temperature, and the elastic modulus of the coating material. The thermal mismatch stress increases with

increasing the difference between spray and room temperature, the difference in the thermal expansion coefficients and the elastic modulus of the coating material [20]. Besides, the thermal mismatch stress may be tensile or compressive stress [21].

2.2 The origin and category of stress during service

TBCs usually operate in harsh environments such as high temperatures, high pressures, and extreme mechanical loads. TBCs may undergo chemical changes such as oxidation and sintering, and withstand external loads such as particle erosion and CaO-MgO-Al_2O_3-SiO_2 (CMAS) corrosion, as shown in **Figure 4**. The composition, microstructure and properties may change dynamically. The stress state may also evolve, and the internal crack may appear and propagate, leading to the failure behaviors such as fracture, delamination and even spalling [2, 22].

During service, the aluminum element in the bond coat may continuously diffuse to the interface between the bond coat and the TGO, and react with oxygen entering from the external environment to generate α-Al_2O_3. In this process, TGO gradually grows thicker. Due to the constraint of the upper ceramic top coat and the lower bond coat, the volume expansion caused by the thickening of TGO is limited. A large compressive growth stress in TGO thereby generates [23]. Besides, the thermal expansion coefficient mismatch of the various layers may also produce high residual compressive stresses in TGO during cooling from the service to room temperature. It is found that the compressive stress in TGO can reach 3-6GPa at room temperature [24]. TGO is subjected to large in-plane compression, and tends to undergo elongation or bending deformation in order to release stress. At high temperatures, the plasticity of the bond coat will increase, and creep even may occur. In addition, there are usually many defects at the interface between the ceramic top coat and TGO. During service, TGO may have an out-of-plane displacement into the bond coat at these defects. The compressive stress in TGO may release, resulting in redistribution of stress. The out-of-plane displacement may cause out-of-plane stress in TBCs, leading to crack initiation, crack propagation, and eventual delamination damage [2, 4, 25]. The stress evolution in TGO plays a crucial role in the TBCs failure, and is one of the most important incentives for delamination failure [26].

When TBCs operate in high temperature environments, the ceramic top coat material may sinter. The sintering may cause the voids between the sheet structures and the cracks in the sheet structures to heal, resulting in a significant increase in the stiffness of the ceramic top coat. The changes in the mechanical properties may
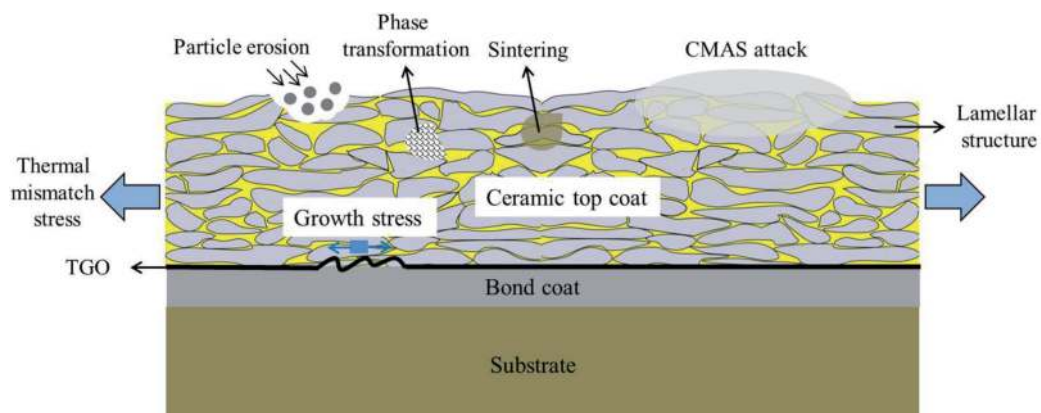

Figure 4.
The factors affecting the stress among APS-prepared TBCs during service.

lead to the change in residual stress. Particularly, the thermal mismatch stress may increase with increasing the modulus, thereby promoting the occurrence of failure [27]. When the temperature is higher than 1200°C, the non-equilibrium metastable phase of 7YSZ may transform into tetragonal phase and monoclinic phase. Large volume deformation may occur in the process of transforming into monoclinic phase, leading to the change in the stress state of TBCs [2].

In some service areas, such as Middle East, silicon-containing debris may enter the engine and melt on the concave (hot side) of the blade. The main component of the melt is CaO-MgO-Al_2O_3-SiO_2, which is called CMAS [2, 28]. When the surface temperature of TBCs exceeds the melting point of CMAS (1240°C), CMAS will infiltrate into the microcracks and voids in TBCs and chemically react with the ceramic top coat material. During the shutdown process of the engine, the ceramic top coat after CMAS infiltration will quickly solidify into a dense layer. The strain tolerance of the top coat will decrease, and the stiffness will increase, increasing the thermal mismatch stress in TBCs [28, 29].

Besides, solid particles in air may also enter the engine, impacting TBCs at high speed during service. The erosion of high speed particles may change the stress state in TBCs [30]. The erosion of the particles produces tensile stress in certain regions of TBCs. Defects such as sheet-like structural interfaces and microcracks in these regions may develop into macroscopic cracks under tensile stress. And macroscopic crack propagation will eventually lead to the spalling of TBCs [31].

3. The measurement technology and characterization method for stress among the APS-prepared TBCs

The stress plays an important role in the failure of the APS-prepared TBCs. It is important to test and characterize the stress. Up to now, various testing techniques and characterization methods for stress among the APS-prepared TBCs have been developed. According to the working principles, the methods can be divided into physical and mechanical testing methods.

3.1 Physical testing methods

In the physical testing methods, the information obtained from the interaction (including diffraction, scattering, etc.) between electromagnetic or particle radiation and the material is used to evaluate the stress distribution in the material. The common physical testing methods mainly include X-ray diffraction, neutron diffraction, Raman spectroscopy, photoluminescence piezospectroscopy and so on.

3.1.1 X-ray diffraction (XRD)

The stress in the coating may cause the crystal plane spacing to change. When X-ray are incident on the coating at different angles, the diffraction angle changes with the incidence angle, which results from the change in the crystal plane spacing. And the change value is related to the stress [32]. In XRD method, X-rays are incident on the surface of the coating at different angles several times, and the changes in the diffraction angle value 2θ are measured, as shown in **Figure 5** [18]. The stress σ can be obtained by calculating the slope of 2θ versus $\sin2\psi$, as follows:

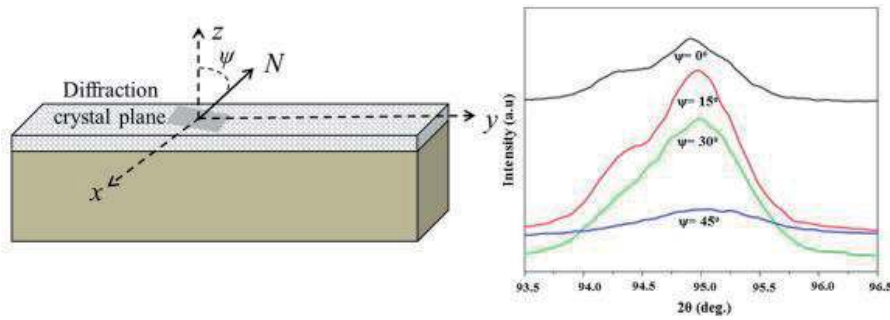$$\sigma = K\frac{d(2\theta)}{d(\sin^2\psi)} \tag{3}$$

Figure 5.
The schematic diagram for measuring stress by XRD.

where, ψ is the angle between the normal direction of the diffraction crystal plane and coating surface. K are elastic constants.

XRD, as a fast and reliable non-destructive testing technology, has no specific requirements on sample size and shape and is suitable for micro-area stress measurement. It has been widely used in the testing and characterization of stress among TBCs. XRD has been used to study the stress evolution in the ceramic top coat and bond coat after operating at different conditions [33–35]. Meanwhile, Xiao et al. studied the stress evolution of the bond coat during oxidation at 1150°C for different time based on XRD. It was found that the stress in the bond coat mainly generated during the process of cooling from 1150 to 600°C. This may be due to that the β phase deposition during cooling changes the volume of the bond coat [34, 35].

Although XRD has been widely used to test stress among TBCs, the penetration depth of X-ray generated by laboratory sources is limited to only a few tens of microns. And the thickness of the coating ranges from 300 to 500 μm. Thus, XRD can only measure the stress state of the near surface zone and not characterize the stress state deep inside TBCs [36].

In order to overcome the problem for small penetration depth of X-ray generated by laboratory sources, synchrotron radiation XRD has been developed. The X-ray generated by synchrotron radiation source is used to test the stress deep inside the material. Comparing with the X-ray generated by the laboratory source, the penetration ability is greatly enhanced [19]. The composition of the local phase and the stress deep inside the thermal spray coating were determined by synchrotron radiation XRD [36]. However, the synchrotron radiation device with the large size, high cost, limited machine time is difficult to promote in the laboratory. The application of synchrotron radiation XRD is limited.

3.1.2 Neutron diffraction

Neutrons with a strong penetrating ability (up to a few tens of millimeters), can penetrate through most materials. Neutron diffraction can be used to measure stress deep inside TBCs, whose principle is basically similar to XRD. The stress distribution in the depth direction of the coating was studied by neutron diffraction. The influence of various operation conditions on the stress distribution was discussed [37, 38]. Neutron diffraction is also suitable for measuring the stress in a large specimen and obtaining the average stress inside the specimen. However, during neutron diffraction testing, the position of the surface with respect to the neutron beam must be accurately known. The 'center of gravity' of a near-surface gauge measurement volume must be calculated. A correction may be required to allow for any pseudostrain effects. Besides, sufficient data are difficult to obtain in a limited time using a weak neutron source, and a special strong neutron source is generally required [38].

3.1.3 Raman spectroscopy

When the laser with a certain frequency is incident on the material, the molecules in the material absorb part of the energy, vibrate in different ways and degrees, and scatter light with a lower frequency. This phenomenon is called Raman scattering. After the incident photons collide with the molecules, the vibrational energy or the rotational energy of the molecules and the photon energy superimpose each other to form a Raman spectrum. When there is stress in the material, some stress-sensitive bands may move and deform relative to the stress-free state, and the position of the spectral peak also may move, as shown in **Figure 6** [39]. It is found that there is a linear relationship between Raman frequency shift and the stress. The frequency shift of the spectral peak can be expressed as:

$$\Delta\omega = \Pi_{ij}\sigma_{ij} \tag{4}$$

where, Π_{ij} is the piezospectroscopic tensor, which represents the stress sensitivity of Raman band. σ_{ij} refers to the stress tensor. $\Delta\omega = \omega_s-\omega_o$, with ω_o being the peak position of the stress-free state and ω_s being the peak position of the stressed state. Then, the stress value can be obtained by measuring the positions of the Raman spectrum peak when the material is stressed or not.

Raman spectroscopy has been widely used to test and characterize stress among APS-prepared TBCs [40]. It is well known that stress in TBCs is inevitably generated during the preparation process. Therefore, it is difficult to obtain a TBCs specimen coated on the substrate in a stress-free state. Generally, a TBCs specimen without the substrate is chosen as a test piece for stress-free conditions. First, the laser with a certain frequency is incident on the TBCs specimen without the substrate to obtain a Raman spectrum (labeled as spectrum 1) corresponding to a stress-free state. Then, a known external stress is applied on the TBCs specimen without the substrate, and the measured Raman spectrum is labeled as spectrum 2. By comparing the spectrum 1 and 2, the piezospectroscopic tensor of TBCs can be obtained according to Eq. (4). Finally, the laser with the same frequency is incident on the TBCs specimen with the substrate, and Raman spectrum, which is labeled as spectrum 3, is obtained. By comparing the spectrum 1 and 3, the stress state in TBCs with the substrate can be evaluated combining the piezospectroscopic tensor obtained above [39, 40].
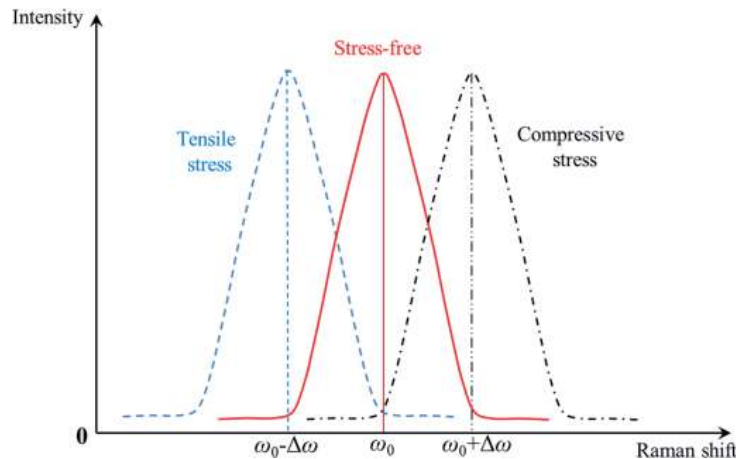

Figure 6.
The schematic diagram for measuring stress by Raman spectroscopy.

TBCs is generally constructed of porous structures for thermal insulation. When the laser is incident on the porous region, the signal intensity will decrease rapidly due to the optical focus limitation of the instrument. In order to reduce the occurrence of the above phenomenon, the incident position of the laser is set in the dense region to obtain the maximum signal intensity, thereby reducing the influence of voids and cracks [40]. Raman spectroscopy, as a non-destructive, non-contact stress testing method, has many advantages such as high spatial resolution, large spectral range, and so on. Besides, it can measure the stress in the depth direction by adjusting the focusing parameters. However, Raman spectral peak shift is susceptible to external factors such as focus depth, laser heating effect, temperature stability, and so on. And high precision is difficult to achieve without effective calibrations. Besides, as the spot of the laser is generally small to obtain high intensity, it is impossible to measure the stress in a large area. Only local stress information can be obtained.

3.1.4 Photoluminescence piezospectroscopy

Since the TGO (mainly composed of α-Al_2O_3) usually contains a trace amount of Cr^{3+}, the ion may generate fluorescence under laser excitation, and its characteristic fluorescence spectrum is bimodal R_1 and R_2. Similar to the Raman spectroscopy, stress can also lead to changes in the peak frequencies of R_1 and R_2 spectrum. The stress value in the TGO can be obtained by measuring the change in the peak frequency of the fluorescence spectrum under stress. The above method is called as photoluminescence piezospectroscopy [41, 42].

Up to now, photoluminescence piezospectroscopy is mainly applied to the EB-PVD prepared TBCs. The laser easily penetrates the columnar crystal structure, and the reflected signals are strong. However, the scattering of pores and grain boundaries in the APS-prepared TBCs may weaken reflection signals and make it difficult to perform spectral analysis.

3.2 Mechanical testing methods

In the mechanical testing methods, the mechanical information such as displacement and strain of the coating system under certain operating or external excitation conditions is measured. Based on the theoretical model, the stress distribution in the coating can be evaluated. The common mechanical testing methods include curvature measurement, material removal, indentation and so on.

3.2.1 Curvature measurement method

During the preparation process or service, the deformation of the coating is limited by the substrate, and an interaction force is generated between the substrate and the coating. Meanwhile, a bending moment appears to bend the overall structure, and curvature occurs to balance the stress in TBCs. The curvature of the substrate is measured by optical or mechanical methods. By analyzing the change in the curvature of the substrate, the stress evolution of TBCs can be derived. The curvature measurement method was first proposed by Stoney [43] and later applied to APS-prepared coatings. Kuroda et al. [44] developed an in-situ curvature monitoring method. In this method, the stress evolution of TBCs during preheating, spraying and cooling process were monitored. The quenching stress during the spraying process and thermal mismatch stress during the cooling process were obtained, as shown in **Figure** 7. In the spraying process, the thickness of the coating gradually increases, and the curvature of the substrate also changes continuously. According to the equilibrium conditions, the quenching stress can be calculated.
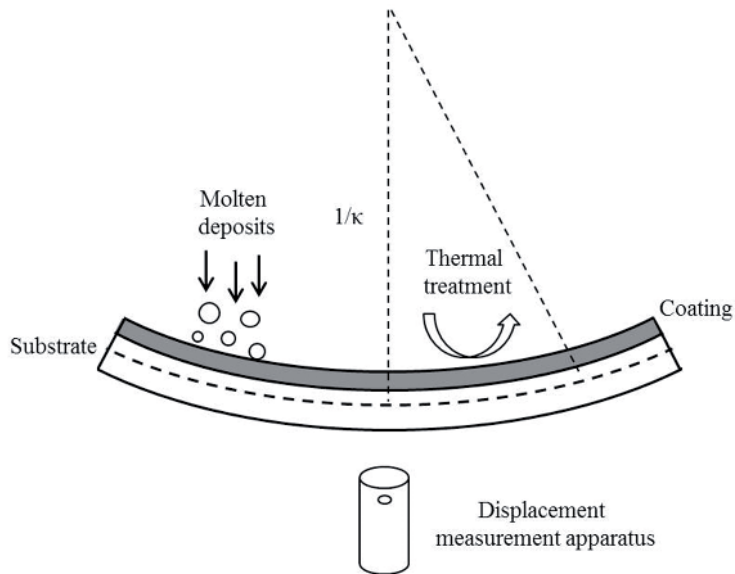
9

Figure 7.
The schematic diagram for measuring stress by curvature measurement method.

In the cooling process, the thermal mismatch strain between the coating and substrate changes the curvature of the substrate. Then, the thermal mismatch stress can be estimated. Besides, the complicated service loads also lead to the change in the curvature of the substrate. The stress evolution in service can also be obtained by the curvature measurement method [20, 39, 45].

In the curvature measurement method, the substrate deformation of the single point or multiple points is measured by the displacement measurement method. According to the geometric relationship, the curvature is calculated. The stress value can also be obtained based on the equilibrium equations. There are two key problems in the curvature measurement method: one is the accurate measurement of deformation, and the other is the accurate calculation of stress.

Many methods have been developed to measure the deformation, mainly including contact measurement and non-contact measurement method. In the contact measurement method, the deformation at specific point is measured by the high-precision contact displacement sensors, such as extensometers, linear variable differential transformer and so on [46, 47]. In the non-contact measurement method, the deformation of the substrate is measured by a non-contact displacement measuring device, such as laser displacement sensor, optical microscope, CCD camera, and so on [48, 49]. For example, during the measurement of deformation by a laser displacement sensor. The laser was incident on the surface of the curved substrate. And deformations at regular intervals were measured. Since the deformation (a few microns) was much smaller than the length of the specimen (a few centimeters), the contour of the substrate was approximated as a parabola or arc. The deformation values were fitted to a parabolic or circular equation according to the least squares method. The curvature of the specimen was calculated based on the above equations. This method has higher accuracy compared to simply measuring the deformation of the middle or end position of the specimen [48].

Once the curvature of the substrate is determined, the stress distribution in the coating can be determined according to the equilibrium equation. The relationship between the curvature and stress of film established by Stoney has been widely used in the stress measurement of film system [43]. However, for thicker coating and multilayer film system, the application of the above relationship is controversial. Clyne

et al. proposed a two-layer beam (or plate) bending model [14]. The relationship between the curvature change $\Delta\kappa$ and the coating average stress σ_r can be given by:

$$\sigma_r = \Delta\kappa \frac{E_c^2 h_c^4 + 4E_c E_s h_c^3 h_s + 6E_c E_s h_c^2 h_s^2 + 4E_c E_s h_c h_s^3 + E_s^2 h_s^4}{6h_s(1-v)E_s h_s(h_c+h_s)} \qquad (5)$$

where, E_c and E_s are the modulus of the coating and substrate, respectively. h_c and h_s are the thickness of the coating and substrate, respectively. v is the Poisson's ratio of the coating. During the preparation process and service, the material properties change with temperature. Clyne et al. considered the influence of temperature on the material properties and obtained more accurate stress values. In order to measure the curvature accurately, test specimens with regular shape such as beam shape and plate shape are chosen in the curvature measurement method. The stress measurement of the test specimens with irregular shape was limited. Besides, the average stress of the coating is obtained from curvature measurement results. More stress information inside the coating is difficult to get.

3.2.2 Material removal method

In the material removal method, the stress state is obtained by monitoring the strain change at a specific position before and after removing the material. The common measurement methods for APS-prepared TBCs include hole-drilling and layer-removal method.

3.2.2.1 Hole-drilling method

In the hole-drilling method, some of the stress-bearing material is removed by drilling holes in the surface of the material. The stress in the remaining material will be redistributed, resulting in a change in the shape of the circular hole. The deformation of the remaining material near the circular hole is measured by strain gauge rosette. The strain distribution can be calculated according to analytical models, and stress distribution can also be estimated [50]. In order to accurately measure the strain change caused by drilling, a specially designed strain gauge rosette is arranged around the drilling point, and the center of the strain gauge rosette should coincide with the drilling point. By analyzing the stress state at the circular hole, the strain measured by different strain gauges can be expressed as:

$$\varepsilon_i = A(\sigma_{max} + \sigma_{min}) + B(\sigma_{max} - \sigma_{min})\cos(2\alpha_i) \qquad (6)$$

where, A and B are calibration coefficients, which are related to parameters such as elastic modulus, Poisson's ratio, and radius of the hole. σ_{max} and σ_{min} are maximum principal and minimum principal stress, respectively. α_i is the angle between the axis of strain gauge and the principal stress axis. By measuring the strains in different directions around the circular hole, the maximum principal and the minimum principal stress at the circular hole can be calculated by Eq. (6). Then the stress state at the circular hole can be estimated. It is worth noting that only when the hole is a through hole and the stress distribution is uniform, A and B have analytical solutions. There are only numerical solutions in the case where the hole is a blind hole or the stress distribution is non-uniform.

As the stress distribution among the APS-prepared TBCs is not uniform, it is recommended to gradually measure the stress distribution in the thickness direction with the incremental hole drilling depth. Then, the drilling method can be developed to the incremental hole drilling method. In this method, the drilling process

is performed in the form of a small step at a time, and the strain changes caused by each step can be recorded by the strain gauges. It is found that after the first drilling step the measured strain changes were affected by both the current and previous small drilling steps [17, 51, 52]. Meanwhile, the calibration coefficients A and B are also related to the drilling depth increment.

Many theoretical studies have been conducted on the incremental hole drilling method. Among them, the integral method can accurately obtain the stress distribution at each drilling step, accounting for the influence of the current and previous small drilling steps. Thus, the integration method is particularly effective for non-uniform stress distribution, especially when the stress changes abruptly with thickness. The stress gradient in the thickness direction can be calculated [53, 54]. However, it is not easy to analyze strain data by the integral method. Numerical methods are usually required. A general method for calculating calibration coefficients based on the finite element method was developed, and the calibration coefficients were obtained accurately [55].

It is worth noting that the above theories are mostly based on the linear elastic model. But the coating may undergo plastic deformation or cracking damage during the drilling process. The stress value calculated by the above theories may deviate from the true value.

3.2.2.2 Layer-removal method

Similar to the hole-drilling method, the layer-removal method also measures the strain change caused by the material reduction to analyze the stress state of the material. But the layer-removal method mainly removes the coating material of a specific thickness by mechanical methods such as grinding and polishing or chemical methods such as corrosion. The physical or mechanical testing methods are used to measure the strain change at a specific position of the remaining material. Then the stress state in the coating can be evaluated [56, 57].

Similarly, if plastic deformation or damage occurs during the removal of the coating material, the linear elastic assumption in the theoretical analysis will no longer be suitable. Besides, it is difficult to remove the same thickness of material each time, especially when the specimen has deformed before the removal of material.

3.2.3 Indentation method

The indentation method, as a common micro-scale mechanical testing method, has been widely used to study the stress in the material. The indentation method mainly includes the nanoindentation and indentation fracture method.

3.2.3.1 Nanoindentation method

It is found that the stress in the materials may lead to the change in the load-displacement curve obtained from the nanoindentation tests. In the indentation method, the tensile stress in the material increases the indentation depth (when the indentation load is chosen) or decreases the indentation load (when the indentation depth is chosen). The compressive stress in the material decreases the indentation depth (when the indentation load is chosen) or increases the indentation load (when the indentation depth is chosen), as shown in **Figure 8**. Then, an indentation method was proposed by Suresh et al. to measure the stress in the materials [58].

Assuming that the stress in the material is an equal-biaxial state, the relationship between the contact area A_0 in a stress-free state and the contact area A under the stress σ_R can be obtained based on the superposition principle, as follows:

$$\frac{A}{A_0} = \left(1 - \frac{\sigma^R \sin\alpha}{H}\right)^{-1} \tag{7}$$

where, H is the indentation hardness. α is the angle between the cone surface of the equivalent conical indenter and the surface of the material (for the Vickers indenter, $\alpha = 22°$; for the Berkovich indenter, $\alpha = 24.7°$).

In the nanoindentation method, indentation tests are conducted on the coating material in the stress-free and stress state, respectively. After indentation load is chosen, the contact areas in the loading stage under the stress-free and stress conditions can be obtained from the load-displacement curves. Then the stress in the material can be evaluated according to Eq. (7) [9, 59, 60].

Two kinds of coating materials corresponding to a stress-free and stress state are required in this method. As mentioned earlier, it is difficult to obtain a TBCs specimen coated on the substrate in a stress-free state. Besides, the nanoindentation method usually has high requirements on the surface quality of the material. But the APS-prepared TBCs is mostly porous, which limits the application of the nanoindentation method.

3.2.3.2 Indentation fracture method

In addition to the elastic-plastic behavior of materials, the indentation method can also be used to study the fracture behavior. When the indentation load is large enough, the stress intensity factor will be larger than the fracture toughness of the material, and the fracture will occur, as shown in **Figure 9**. The fracture toughness of the material can be calculated based on the critical conditions. The stress intensity factor K_s in the stress-free state can be expressed as:

$$K_s = \delta \left(\frac{E}{H}\right)^{1/2} \frac{P}{c^{3/2}} \tag{8}$$

where, δ is a geometric parameter, which is related with the shape of the indenter. E and H are the modulus and hardness of the material, respectively. P is the indentation load. c is the average length of the cracks induced by indentation.
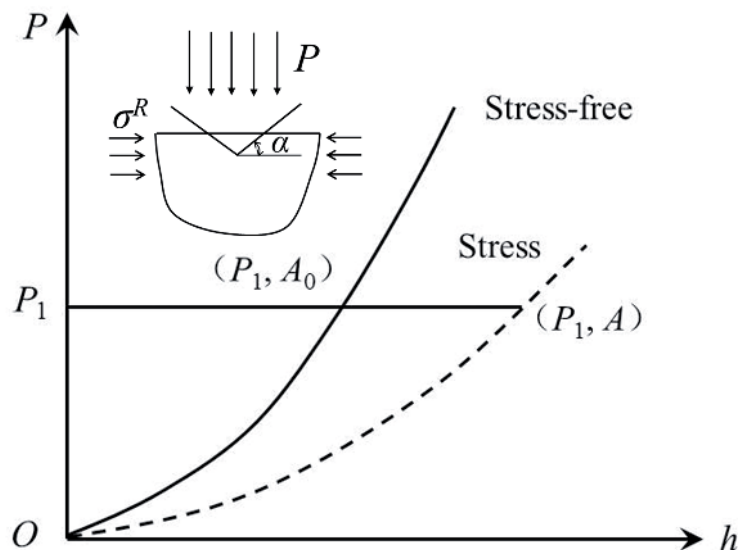
Figure 8.
The schematic diagram for measuring stress by nanoindentation method.
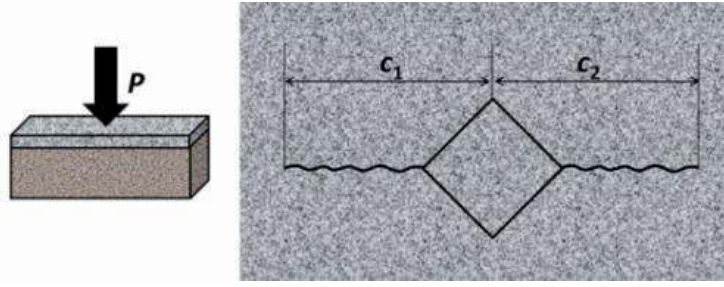
Figure 9.
The schematic of indentation fracture.

The stress in the material may influence the critical load corresponding to the occurrence of facture. Tensile stress promotes the initiation and propagation of cracks. When the stress in the material is tensile, the critical load decreases. Compressive stress inhibits the initiation and propagation of cracks. When the stress in the material is compressive, the critical load increases. Assuming that the stress σ_r in the coating is uniform, the contribution of stress to the stress intensity factor K_r can be expressed as:

$$K_r = \psi \sigma_r \sqrt{t}\left(2 - \sqrt{t/c}\right) \tag{9}$$

where, t is the thickness of the coating. $\psi = 2/\sqrt{\pi}$ is crack geometric parameter.

Based on the superposition principle, combing Eq. (8) and (9), the total stress intensity factor K can be expressed as:

$$K = \delta \left(\frac{E}{H}\right)^{1/2} \frac{P}{c^{3/2}} + 2\psi\sigma_r t^{1/2} - \psi\sigma_r t/c^{1/2} \tag{10}$$

When the stress intensity factor is larger than the fracture toughness K_{IC} of the material, the fracture will occur. According to the critical conditions, Eq. (10) can be rewritten as:

$$\frac{P}{c^{3/2}} = \frac{K_{IC} - 2\psi\sigma_r t^{1/2}}{\chi} + (\psi\sigma_r t)\,c^{-1/2} \tag{11}$$

where $\chi = \delta(E/H)^{1/2}$.

According to Eq. (11), there is linear relationship between $P/c^{3/2}$ and $c^{-1/2}$. $\psi\sigma_r t$ and $K_{IC}-2\psi\sigma_r t^{1/2}$ represent the slope and intercept, respectively. Therefore, the indentation fracture tests under different indentation loads need to be conducted. The crack lengths under different indentation loads are measured. By linear fitting, the slope and intercept values can be obtained. Then the residual stress and fracture toughness of the material can be evaluated [61]. The indentation fracture method has been successfully used to measure and analyze the stress in ceramic top coat and at the interface between the ceramic top and the bond coat. [33, 62]. Besides, the indentation fracture method has also been extended to the high temperature environments. The stress evolution behavior at different service temperatures was studied [63].

As TBCs is a porous non-uniform structure, the process of inducing cracks by indentation is random. The cracks are susceptible to microstructures such as voids, and the data are discrete, which provides difficulties for subsequent data analysis. Generally, a large of experiential results is required.

4. Conclusions and future directions

Up to now, many testing techniques and characterization methods for stress among APS-prepared TBCs have been developed. The stress in the ceramic top coat, TGO and bond coat under various operating conditions were obtained. However, some topics, such as the measurement of the stress deep inside TBCs, the in-situ evaluation of the stress among TBCs applied on the profiled blade, and the real-time monitoring of the stress among TBCs under the complicated service environments have yet to be further studied. Thus, for the testing of stress among APS-prepared TBCs, the following aspects should be considered in the future:

1. The APS-prepared TBCs has complicated microstructure, and internal stress distribution is non-uniform. Existing laboratory testing techniques only non-destructively measure the stress state of the near surface zone. In order to non-destructively measure the stress deep inside the coating, large scientific equipment is required, which has a lot of limitations. It is necessary to further develop the non-destructive testing technology and characterization method of the stress deep inside the TBCs to realize the analysis of the stress in all zones.

2. The existing testing specimens for the measurement of stress among TBCs are mostly custom-made regular shape specimens and generally cut from the actual profiled blade. The cutting process may affect the stress inside the coating. Besides, the change in the shape of the substrate may also affect the stress in the coating, resulting in the measured stress deviating from the actual stress. Thus, it is necessary to develop testing techniques for the stress among the TBCs coated on profiled substrate. Special attention should be given to a portable testing instrument for in situ non-destructive stress measurement.

3. The existing testings on stress among the TBCs are mostly conducted at room temperature. The residual stress states in the TBCs were obtained. However, TBCs usually operates under high temperature oxidation environments, and the stress state is different from that at room temperature. The testing and characterization of stress under high temperature oxidation environment are also of great significance for the failure mechanism analysis of TBCs. It is necessary to develop testing techniques and characterization methods for the stress among TBCs under high temperature oxidation environments. The study on real-time monitoring of stress among TBCs during service should be conducted.

Acknowledgements

Conflict of interest

The authors declared that they have no conflicts of interest to this work.

Author details

Zhaoliang Qu*, Rujie He and Daining Fang
Beijing Institute of Technology, Beijing, China

*Address all correspondence to: quzl@bit.edu.cn

IntechOpen

References

[1] Padture N, Gell M, Jordan E. Thermal barrier coatings for gas-turbine engine applications. Science. 2002;**296**(5566):280-284. DOI: 10.1126/science.1068609

[2] Darolia R. Thermal barrier coatings technology: Critical review, progress update, remaining challenges and prospects. International Materials Reviews. 2013;**58**(6):315-348. DOI: 10.1179/1743280413Y.0000000019

[3] Levi C. Emerging materials and processes for thermal barrier systems. Current Opinion in Solid State and Materials Science. 2004;**8**(1):77-91. DOI: 10.1016/j.cossms.2004.03.009

[4] Evans A, He M, Hutchinson J. Mechanics-based scaling laws for the durability of thermal barrier coatings. Progress in Materials Science. 2001;**46**(3-4):249-271. DOI: 10.1016/S0079-6425(00)00007-4

[5] Vaßen R, Jarligo M, Steinke T, Mack D, Stöver D. Overview on advanced thermal barrier coatings. Surface and Coatings Technology. 2010;**205**(4):938-942. DOI: 10.1016/j.surfcoat.2010.08.151

[6] Kumar V, Kandasubramanian B. Processing and design methodologies for advanced and novel thermal barrier coatings for engineering applications. Particuology. 2016;**27**:1-28. DOI: 10.1016/j.partic.2016.01.007

[7] Hardwicke C, Lau Y. Advances in thermal spray coatings for gas turbines and energy generation: A review. Journal of Thermal Spray Technology. 2013;**22**(5):564-576. DOI: 10.1007/s11666-013-9904-0

[8] Kumar V, Balasubramanian K. Progress update on failure mechanisms of advanced thermal barrier coatings: A review. Progress in Organic Coatings. 2016;**90**:54-82. DOI: 10.1016/j.porgcoat.2015.09.019

[9] Zhu J, Xie H, Hu Z, Chen P, Zhang Q. Cross-sectional residual stresses in thermal spray coatings measured by moiré interferometry and nanoindentation technique. Journal of Thermal Spray Technology. 2012;**21**(5):810-817. DOI: 10.1007/s11666-012-9732-7

[10] He M, Hutchinson J, Evans A. Simulation of stresses and delamination in a plasma-sprayed thermal barrier system upon thermal cycling. Materials Science and Engineering A. 2003;**345**(1-2):172-178. DOI: 10.1016/S0921-5093(02)00458-6

[11] Qu Z, Cheng X, Wu J, He R, Pei Y, Fang D. An investigation on erosion behavior of nanostructured 7YSZ coatings at elevated temperature. Surface and Coatings Technology. 2016;**299**:129-134. DOI: 10.1016/j.surfcoat.2016.05.003

[12] Golosnoy I, Cipitria A, Clyne T. Heat transfer through plasma-sprayed thermal barrier coatings in gas turbines: A review of recent work. Journal of Thermal Spray Technology. 2009;**18**(5-6):809-821. DOI: 10.1007/s11666-009-9337-y

[13] Clyne T, Gill S. Residual stresses in thermal spray coatings and their effect on interfacial adhesion: A review of recent work. Journal of Thermal Spray Technology. 1996;**5**(4):401

[14] Tsui Y, Clyne T. An analytical model for predicting residual stresses in progressively deposited coatings. Part 1: Planar geometry. Thin Solid Films. 1997;**306**(1):23-33. DOI: 10.1016/S0040-6090(97)00199-5

[15] Valente T, Bartuli C, Sebastiani M, Loreto A. Implementation and development of the incremental hole drilling method for the measurement of residual stress in thermal spray

coatings. Journal of Thermal Spray Technology. 2005;**14**(4):462-470. DOI: 10.1361/105996305X76432

[16] McPherson R. The relationship between the mechanism of formation, microstructure and properties of plasma-sprayed coatings. Thin Solid Films. 1981;**83**(3):297-310. DOI: 10.1016/0040-6090(81)90633-7

[17] Kuroda S, Fukushima T, Kitahara S. Significance of quenching stress in the cohesion and adhesion of thermally sprayed coatings. Journal of Thermal Spray Technology. 1992;**1**(4):325-332

[18] Matejicek J, Sampath S, Dubsky J. X-ray residual stress measurement in metallic and ceramic plasma sprayed coatings. Journal of Thermal Spray Technology. 1998;**7**(4):489-496

[19] Ang A, Berndt C. A review of testing methods for thermal spray coatings. International Materials Reviews. 2014;**59**(4):179-223. DOI: 10.1179/1743280414Y.0000000029

[20] Matejicek J, Sampath S. In situ measurement of residual stresses and elastic moduli in thermal sprayed coatings. Part 1: Apparatus and analysis. Acta Materialia. 2003;**51**(3):863-872. DOI: 10.1016/S1359-6454(02)00478-0

[21] Matejicek J, Sampath S. Intrinsic residual stresses in single splats produced by thermal spray processes. Acta Materialia. 2001;**49**(11):1993-1999. DOI: 10.1016/S1359-6454(01)00099-4

[22] Chen X, He M, Spitsberg I, Fleck N, Hutchinson J, Evans A. Mechanisms governing the high temperature erosion of thermal barrier coatings. Wear. 2004;**256**(7-8):735-746. DOI: 10.1016/S0043-1648(03)00446-0

[23] Rabiei A, Evans A. Failure mechanisms associated with the thermally grown oxide in plasma-sprayed thermal barrier coatings. Acta Materialia. 2000;**48**(15):3963-3976. DOI: 10.1016/S1359-6454(00)00171-3

[24] Lipkin D, Clarke D. Measurement of the stress in oxide scales formed by oxidation of alumina-forming alloys. Oxidation of Metals. 1996;**45**(3-4): 267-280. DOI: 10.1007/BF01046985

[25] Hutchinson J, He M, Evans A. The influence of imperfections on the nucleation and propagation of buckling driven delaminations. Journal of the Mechanics and Physics of Solids. 2000;**48**(4):709-734. DOI: 10.1016/S0022-5096(99)00050-2

[26] Cheruvu N, Chan K, Viswanathan R. Evaluation, degradation and life assessment of coatings for land based combustion turbines. Energy Materials. 2006;**1**(1):33-47. DOI: 10.1179/174892306X99705

[27] Cipitria A, Golosnoy I, Clyne T. A sintering model for plasma-sprayed zirconia thermal barrier coatings. Part II: Coatings bonded to a rigid substrate. Acta Materialia. 2009;**57**(4):993-1003. DOI: 10.1016/j.actamat.2008.10.058

[28] Krämer S, Faulhaber S, Chambers M, Clarke D, Levi C, Hutchinson J, et al. Mechanisms of cracking and delamination within thick thermal barrier systems in aero-engines subject to calcium-magnesium-alumino-silicate (CMAS) penetration. Materials Science and Engineering A. 2008;**490**(1-2): 26-35. DOI: 10.1016/j.msea.2008.01.006

[29] Krause A, Garces H, Dwivedi G, Ortiz A, Sampath S, Padture N. Calcia-magnesia-alumino-silicate (CMAS)-induced degradation and failure of air plasma sprayed yttria-stabilized zirconia thermal barrier coatings. Acta Materialia. 2016;**105**:355-366. DOI: 10.1016/j.actamat.2015.12.044

[30] Janos B, Lugscheider E, Remer P. Effect of thermal aging on the erosion resistance of air plasma sprayed

zirconia thermal barrier coating. Surface and Coatings Technology. 1999;**113**(3):278-285. DOI: 10.1016/S0257-8972(99)00002-X

[31] Ramachandran C, Balasubramanian V, Ananthapadmanabhan P. Erosion of atmospheric plasma sprayed rare earth oxide coatings under air suspended corundum particles. Ceramics International. 2013;**39**(1):649-672. DOI: 10.1016/j.ceramint.2012.06.077

[32] Noyan I, Huang T, York B. Residual stress/strain analysis in thin films by X-ray diffraction. Critical Reviews in Solid State and Materials Sciences. 1995;**20**(2):125-177. DOI: 10.1080/10408439508243733

[33] Chen Q, Mao W, Zhou Y, Lu C. Effect of Young's modulus evolution on residual stress measurement of thermal barrier coatings by X-ray diffraction. Applied Surface Science. 2010;**256**(23):7311-7315. DOI: 10.1016/j.apsusc.2010.05.071

[34] Chen Y, Zhao X, Dang Y, Xiao P, Curry N, Markocsan N, et al. Characterization and understanding of residual stresses in a NiCoCrAlY bond coat for thermal barrier coating application. Acta Materialia. 2015;**94**: 1-14. DOI: 10.1016/j.actamat.2015.04.053

[35] Yang L, Zou Z, Kou Z, Chen Y, Zhao G, Zhao X, et al. High temperature stress and its influence on surface rumpling in NiCoCrAlY bond coat. Acta Materialia. 2017;**139**:122-137. DOI: 10.1016/j.actamat.2017.08.001

[36] Weyant C, Almer J, Faber K. Through-thickness determination of phase composition and residual stresses in thermal barrier coatings using high-energy X-rays. Acta Materialia. 2010;**58**(3):943-951. DOI: 10.1016/j.actamat.2009.10.010

[37] Scardi P, Leoni M, Bertini L, Bertamini L, Cernuschid F. Strain

gradients in plasma-sprayed zirconia thermal barrier coatings. Surface and Coating Technology. 1998;**108**:93-98. DOI: 10.1016/S0257-8972(98)00616-1

[38] Ahmed R, Yu H, Stoica V, Edwards L, Santisteban J. Neutron diffraction residual strain measurements in post-treated thermal spray cermet coatings. Materials Science and Engineering A. 2008;**498**(1-2):191-202. DOI: 10.1016/j.msea.2008.08.023

[39] Yang L, Yang F, Long Y, Zhao Y, Xiong X, Zhao X, et al. Evolution of residual stress in air plasma sprayed yttria stabilised zirconia thermal barrier coatings after isothermal treatment. Surface and Coatings Technology. 2014;**251**:98-105. DOI: 10.1016/j.surfcoat.2014.04.009

[40] Tanaka M, Hasegawa M, Dericioglu A, Kagawa Y. Measurement of residual stress in air plasma-sprayed Y_2O_3–ZrO_2 thermal barrier coating system using micro-Raman spectroscopy. Materials Science and Engineering A. 2006;**419**(1-2):262-268. DOI: 10.1016/j.msea.2005.12.034

[41] Schlichting K, Vaidyanathan K, Sohn Y, Jordan E, Gell M, Padture N. Application of Cr^{3+} photoluminescence piezo-spectroscopy to plasma-sprayed thermal barrier coatings for residual stress measurement. Materials Science and Engineering A. 2000;**291**(1-2):68-77. DOI: 10.1016/S0921-5093(00)00973-4

[42] Majewski M, Kelley C, Lake J, Renfro M, Hassan W, Brindley W, et al. Stress measurements via photoluminescence piezospectroscopy on engine run thermal barrier coatings. Surface and Coatings Technology. 2012;**206**(11-12):2751-2758. DOI: 10.1016/j.surfcoat.2011.11.026

[43] Stoney G. The tension of metallic films deposited by electrolysis.

Proceedings of the Royal Society A. 1909;**82**(553):172-175

[44] Kuroda S, Fukushima T, Kitahara S. Generation mechanisms of residual stresses in plasma-sprayed coatings. Vacuum. 1990;**41**(4-6):1297-1299. DOI: 10.1016/0042-207X(90)93938-F

[45] Gill S, Clyne T. Investigation of residual stress generation during thermal spraying by continuous curvature measurement. Thin Solid Films. 1994;**250**(1-2):172-180. DOI: 10.1016/0040-6090(94)90182-1

[46] Zhang X, Watanabe M, Kuroda S. Effects of residual stress on the mechanical properties of plasma-sprayed thermal barrier coatings. Engineering Fracture Mechanics. 2013;**110**:314-327. DOI: 10.1016/j. engfracmech.2013.08.016

[47] Dwivedi G, Nakamura T, Sampath S. Determination of thermal spray coating property with curvature measurements. Journal of Thermal Spray Technology. 2013;**22**(8):1337-1347. DOI: 10.1007/ s11666-013-9981-0

[48] Teixeira V, Andritschky M, Fischer W, Buchkremer P, Stöver D. Analysis of residual stresses in thermal barrier coatings. Journal of Materials Processing Technology. 1999;**92**:209-216. DOI: 10.1016/S0924-0136(99)00157-0

[49] Zhu J, Xie H, Hu Z, Chen P, Zhang Q. Residual stress in thermal spray coatings measured by curvature based on 3D digital image correlation technique. Surface and Coatings Technology. 2011;**206**(6):1396-1402. DOI: 10.1016/j.surfcoat.2011.08.062

[50] Schajer G, Yang L. Residual-stress measurement in orthotropic materials using the hole-drilling method. Experimental Mechanics. 1994;**34**(4):324-333

[51] Wu L, Zhu J, Xie H. Numerical and experimental investigation of residual stress in thermal barrier coatings during APS process. Journal of Thermal Spray Technology. 2014;**23**(4):653-665. DOI: 10.1007/s11666-014-0063-8

[52] Santana Y, La Barbera-Sosa J, Staia M, Lesage J, Puchi-Cabrera E, Chicot D, et al. Measurement of residual stress in thermal spray coatings by the incremental hole drilling method. Surface and Coatings Technology. 2006;**201**(5):2092-2098. DOI: 10.1016/j. surfcoat.2006.04.056

[53] Schajer G. Measurement of non-uniform residual stresses using the hole-drilling method. Part I—Stress calculation procedures. Journal of Engineering Materials and Technology. 1988;**110**(4):338-343

[54] Huang X, Liu Z, Xie H. Recent progress in residual stress measurement techniques. Acta Mechanica Solida Sinica. 2013;**26**(6):570-583. DOI: 10.1016/S0894-9166(14)60002-1

[55] Schajer G. Application of finite element calculations to residual stress measurements. Journal of Engineering Materials and Technology. 1981;**103**(2):157-163

[56] Greving D, Rybicki E, Shadley J. Through-thickness residual stress evaluations for several industrial thermal spray coatings using a modified layer-removal method. Journal of Thermal Spray Technology. 1994;**3**(4):379

[57] Lima C, Nin J, Guilemany J. Evaluation of residual stresses of thermal barrier coatings with HVOF thermally sprayed bond coats using the modified layer removal method (MLRM). Surface and Coatings Technology. 2006;**200** (20-21):5963-5972. DOI: 10.1016/j. surfcoat.2005.09.016

[58] Suresh S, Giannakopoulos A. A new method for estimating residual stresses

by instrumented sharp indentation.
Acta Materialia. 1998;**46**(16):5755-5767.
DOI: 10.1016/S1359-6454(98)00226-2

[59] Xiao L, Ye D, Chen C. A further
study on representative models for
calculating the residual stress based
on the instrumented indentation
technique. Computational Materials
Science. 2014;**82**:476-482. DOI:
10.1016/j.commatsci.2013.10.014

[60] Atar E, Sarioglu C, Demirler U,
Kayali E, Cimenoglu H. Residual stress
estimation of ceramic thin films by
X-ray diffraction and indentation
techniques. Scripta Materialia.
2003;**48**(9):1331-1336. DOI: 10.1016/
S1359-6462(03)00019-8

[61] Lawn B, Fuller E. Measurement
of thin-layer surface stresses
by indentation fracture.
Journal of Materials Science.
1984;**19**(12):4061-4067

[62] Mao W, Wan J, Dai C, Ding J,
Zhang Y, Zhou Y, et al. Evaluation of
microhardness, fracture toughness
and residual stress in a thermal
barrier coating system: A modified
Vickers indentation technique.
Surface and Coatings Technology.
2012;**206**(21):4455-4461. DOI:
10.1016/j.surfcoat.2012.02.060

[63] Qu Z, Wei K, He Q, He R, Pei Y,
Wang S, et al. High temperature
fracture toughness and residual stress in
thermal barrier coatings evaluated by an
in-situ indentation method. Ceramics
International. 2018;**44**(7):7926-7929.
DOI: 10.1016/j.ceramint.2018.01.230